Synthesis, Optical and Electrochemical Properties of High-Quality Cross-Conjugated Aromatic Polyketones

Ye, Gang; Liu, Yuru; Abdu-Aguye, Mustapha; Loi, Maria A.; Chiechi, Ryan C.

Published in:
ACS Omega

DOI:
10.1021/acsomega.0c00223

Publication date:
2020

ACS OMEGA

http://pubs.acs.org/journal/acsodf

Article

Synthesis, Optical and Electrochemical Properties of High-Quality Cross-Conjugated Aromatic Polyketones

Gang Ye, Yuru Liu, Mustapha Abdu-Aguye, Maria A. Loi, and Ryan C. Chiechi*

Cite This: *ACS Omega* 2020, 5, 4689−4696

Read Online

ACCESS | Metrics & More | Article Recommendations | Supporting Information

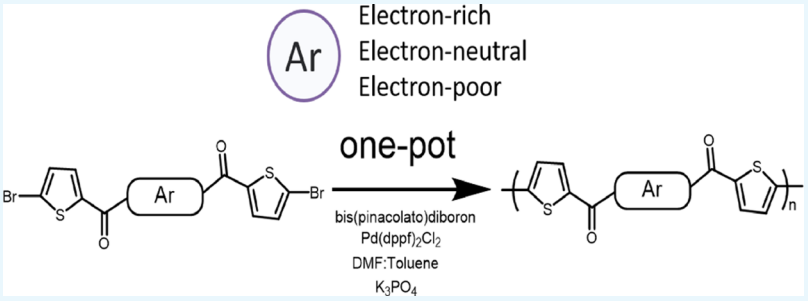

ABSTRACT: This paper describes the synthesis and characterization of three new aromatic polyketones with repeating units based on 2,2′-(2,5-dihexyl-1,4-phenylene) dithiophene (PTK), 2,2′-(9,9-dihexyl-9*H*-fluorene-2,7-diyl)dithiophene (PFTK), and 4,7-bis(3-hexylthiophen-2-yl)benzo[*c*][1,2,5]thiadiazole (PBTK). These polymers were obtained with a one-pot Suzuki−Miyaura cross-coupling-promoted homopolymerization to afford high-quality, defect-free polymers. Experimental and theoretical studies were applied to investigate their optical and electrical properties. The cross-conjugated nature of aromatic polyketones imparts excellent thermal stability. Exposure to acid converts the cross-conjugation to linear-conjugation, enabling the dynamic tuning of optoelectronic properties.

1. INTRODUCTION

Aromatic polyketones, where the backbones are composed of repeating diarylketones, are well-known as high-performance polymers with excellent chemical and physical properties and remarkable thermal stability.[1] These materials have exhibited potential applications as super-engineering plastics.[1−3] However, aromatic polyketones have only recently been investigated as electro-active materials, in particular, as n-type optoelectronic semiconductors.[4,5] Moreover, cross-conjugated aromatic polyketones are useful as precursors to linearly-conjugated polymers with unique properties by the addition of nucleophiles. The resulting polymers, which we refer to as conjugated polyions (CPIs), are pristine semiconductors that bear charges in the backbone, making them processable from polar, protic solvents.[6,7] Although CPIs bear charges in the backbone, they are closed-shell, meaning they do not act as polarons, and the polymers, therefore, remain in a semiconducting state. These properties cannot be achieved by traditional doping, which is why we sought to develop more robust syntheses for their polyketone precursors.

There are relatively few reports about novel polymerization methods to prepare cross-conjugated aromatic polyketones. Curtis and co-workers developed the synthesis of cross-conjugated aromatic poly(3-alkylthiophene)ketones by a Pd-catalyzed copolymerization of bis(chloromercury)-thiophenes (highly toxic) with carbon oxides (high pressure) in hot pyridine.[8−10] Hudson and co-workers reported the synthesis of aromatic polyketones through an aldol condensation of cyclic ketones with aromatic dialdehydes.[11] However, these aromatic polyketones materials suffered from low solubility because they were partially cross-linked. Gibson and co-workers reported the synthesis of aromatic polyketones via the nucleophilic aromatic substitution between arylene dihalides and dicarbanions derived from bis(α-amino nitrile)s, followed by hydrolysis.[2,3] However, the synthesis of bis(α-amino nitrile)s involved NaCN, and the post-polymerization was hard to achieve high yields and would produce side products. Ito and co-workers reported a palladium-catalyzed alternating copolymerization of formal aryne with carbon monoxide.[12] Subsequent acid-promoted dehydration yielded the new aromatic polyketones. This method produced aromatic polyketones together with the corresponding polyketal isomers. Both band gaps and the absolute energies of molecular orbitals are important parameters to control for organic semiconductors;[13] however, the aforementioned

Received: January 16, 2020
Accepted: February 18, 2020
Published: February 28, 2020

https://dx.doi.org/10.1021/acsomega.0c00223
ACS Omega 2020, 5, 4689−4696

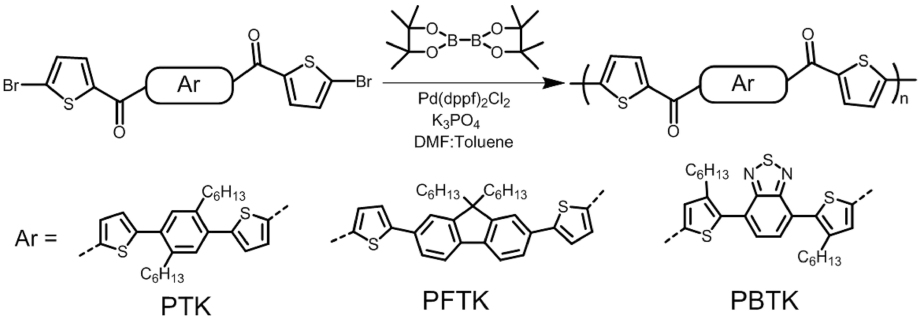

Figure 1. Synthesis of aromatic polyketones via one-pot Suzuki–Miyaura homo-polymerization.

synthetic routes are not targeted at semiconducting properties and thus are limited in the ability to tune these properties in aromatic polyketones.[12] The electrophilic Friedel–Crafts polymerization between bifunctional aromatic acyl chlorides and electron-rich aromatic compounds can generate high-quality aromatic polyketones, but it has a narrow scope of substrates.[14−17] Hence, it is necessary to develop new strategies for the synthesis of aromatic polyketones that allows a broader substrate scope if they are to be developed as semiconducting materials.

Transition metal (palladium or nickel)-catalyzed polymerization promoted by cross-couplings such as Stille and Suzuki–Miyaura couplings have been widely used to construct conjugated polymers, in general. However, there are few reports of a transition metal-catalyzed polymerization method being used to synthesize an aromatic polyketone.[4,18−20] We have previously shown that one-pot borylation/cross-coupling polymerizations are superior to Stille copolymerization for control over end group chemistry.[21,22] Here, we expand the scope of this polymerization method to the synthesis of aromatic polyketones for use as semiconducting materials and precursors to conjugated polyions[23] with the synthesis and characterization of three new aromatic polyketones with electron-neutral (PTK), electron-withdrawing (PBTK), and electron-donating groups (PFTK) in the backbone. These polymers were synthesized with a one-pot Suzuki–Miyaura cross-coupling promoted homopolymerization, which offered good chemical integrity. We systematically investigate the band gap and molecular energy levels of these aromatic polyketones by absorption spectroscopy, cyclic voltammetry, and theoretical calculation. As with conventional conjugated polymers, the aromatic polyketones exhibited tunable optoelectronic properties.

2. RESULTS AND DISCUSSION

2.1. Synthesis and Characterization. The synthetic route of the three aromatic polyketones is shown in Figure 1. The synthesis of carbonyl-containing monomers are shown in the Supporting Information. The polymers (PTK, PBTK, and PFTK) were synthesized via one-pot Suzuki homo-coupling polymerization from the symmetric, bisbromo, ketone-containing monomers. We employed the same polymerization condition for the synthesis of aromatic polyketones as our previous contribution.[21,22] We chose DMF and toluene as polymerization co-solvents because DMF can accelerate standard Suzuki polymerization, and toluene is a good solvent for the resulting polymer. Polymers were obtained by refluxing the polymerization mixture overnight. Impurities and low-molecular-weight fractions were removed by methanol and hexane in a Soxhlet extractor. Finally, the polymers were extracted with chloroform, precipitated in methanol, and further dried under vacuum. Some insoluble solids remained after extracting, likely due to the low solubility of the very high molecular weight fractions. This phenomenon has also been observed in a previous work.[22] The molecular weights of these aromatic polyketones were determined by gel permeation chromatography (GPC) using polystyrene as standards (see Figures S19–S21). The resulting data are shown in Table 1.

Table 1. Molecular Weight and Thermal Properties of PTK, PBTK, and PFTK

polymer	M_n (kg mol^{-1})	M_W (kg mol^{-1})	Đ	T_g (°C)	T_d (°C)	T_m (°C)
PTK	7.3	57.7	7.88	76	380	230
PBTK	6.3	12.7	2.03	100	330	250
PFTK	4.2	7.6	1.83	124	400	225

The M_W values of PTK, PBTK, and PFTK are 57.7, 12.7, and 7.6 kDa, respectively. PFTK and PBTK exhibited moderate distribution with the dispersity index (Đ) values of 1.83 and 2.03, respectively, while PTK showed a broad distribution with a higher value of Đ of 7.88. The high values of Đ could be an indication of an addition polymerization mechanism. Step polymerization reactions typically yield values of Đ around 2.0, whereas chain reactions yield values of Đ between 1.5 and 20. Therefore, it is hard to determine whether this polymerization method is step-growth or chain-growth. (A full investigation of the mechanism of polymerization is beyond the scope of this paper.) The chemical structures of aromatic polyketones were characterized by Fourier transform infrared (FT-IR), ^{1}HNMR, and MALDI-TOF mass spectroscopy. The FT-IR data confirmed the presence/absence of expected/unexpected functional groups in aromatic polyketones. The inclusion of the carbonyl group into the polymer was confirmed by the appearance of the C=O stretching mode around 1600 cm^{-1} in the (FT-IR) spectroscopy, which is shown in the Supporting Information (Figures S16–S18).

The well-resolved peaks in ^{1}HNMR, especially in the aliphatic region, could be viewed as an indication of the high quality and regioregularity of these aromatic polyketones, which are shown in Figures S13–S15. The NMR data (see the Experimental Section) confirmed the connectivity of the polymers, but were not sensitive enough to differentiate the end-groups. The high uniformity and uniform end-groups of these aromatic polyketones are reflected in the MALDI-TOF-MS spectra shown in Figure 2a. As seen in the figure, all spectra show identical repeating peaks, with a repetition interval of 630 Da for PTK, 688 Da for PBTK, and 718 Da for

https://dx.doi.org/10.1021/acsomega.0c00223
ACS Omega 2020, 5, 4689−4696

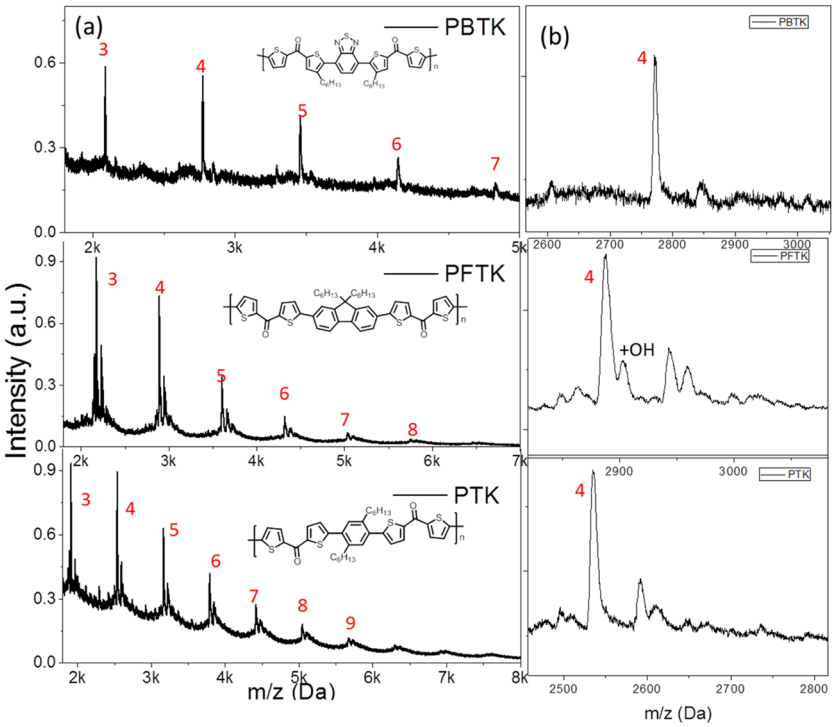

Figure 2. (a) MALDI-TOF spectra of PTK, PBTK, and PFTK. The peaks corresponding to the bis-H-terminated repeating unit (X_n) are labeled with numbers. 2,5-Dihydroxybenzoic acid is used as the matrix for all spectra. (b) Zoom-in of peaks 4 of PTK, PBTK, and PFTK.

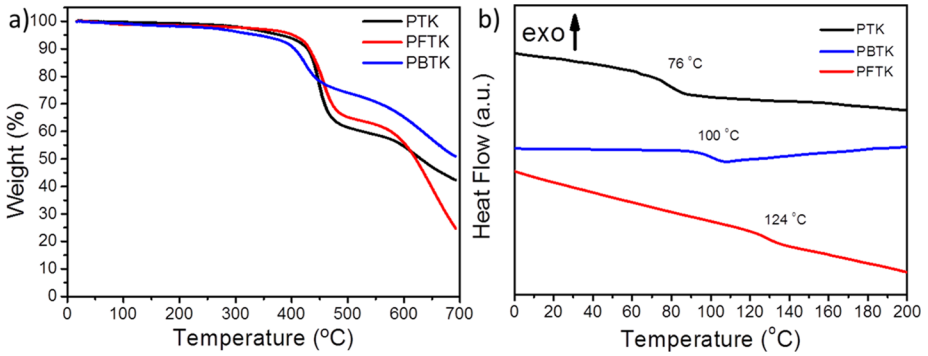

Figure 3. (a) Thermogravimetric analysis plots and (b) DSC curves for PTK, PBTK, and PFTK on second heat, 10 °C/min.

PFTK, respectively, which is consistent with the mass of the monomer unit. In addition, there are no residual Br or boronic ester end groups in all the aromatic polyketones. Some side peaks with higher m/z values around the major peaks are observed as shown in Figure 2b. In PFTK, one of the extra peaks at the tetrameter +17 m/z, might be corresponding to the addition of a hydroxyl group to a polymer chain that transferred from the 2,5-dihydroxybenzoic acid matrix.

2.2. Thermal Properties. The thermal properties of PTK, PBTK, and PFTK were investigated by thermogravimetric analysis (TGA) and differential scanning calorimetry (DSC). The TGA and DSC results are shown in Figure 3, and the corresponding data are summarized in Table 1. All PTK, PBTK, and PFTK showed excellent thermal stability and exhibited a double thermal decomposition process. The decomposition temperature (T_d), where 5% weight loss is reached, is at 380, 330, and 400 °C for PTK, PBTK, and PFTK, respectively. The weight loss of first decomposition step is around 37, 23, and 41 wt % for PTK, PBTK, and PFTK, respectively, which likely correspond to the loss of the hexyl pendant group. The molecular weight ratio of the hexyl pendant group is 39, 20, and 46% for PTK, PBTK, and PFTK, respectively. Given that the high T_d temperatures of these aromatic polyketones, it is reasonable to assume that they can be thermally processed without degradation, which may facilitate their eventual use in organic optoelectronic devices.

The DSC results reveal that these aromatic polyketones are semicrystalline materials. The glass transition temperature (T_g) of PTK, PBTK, and PFTK is at 76, 100, 124 °C, respectively. The increasing T_g from PTK to PBTK to PFTK is consistent with increasing the degree of backbone rigidity of these aromatic polyketones. Moreover, this trend of T_g is also consistent with increasing the degree of PDI these aromatic polyketones. A broad melting endotherm peak was observed at 230 °C for PTK and 250 °C for PBTK, respectively, while the small melting transition was observed for 225 °C PFTK from the full DSC curves (see the Supporting Information, Figures S22−S24). The decreasing melting endotherm trend of aromatic polyketones from PTK to PBTK to PFTK indicates the decrease of crystallinity.

https://dx.doi.org/10.1021/acsomega.0c00223
ACS Omega 2020, 5, 4689−4696

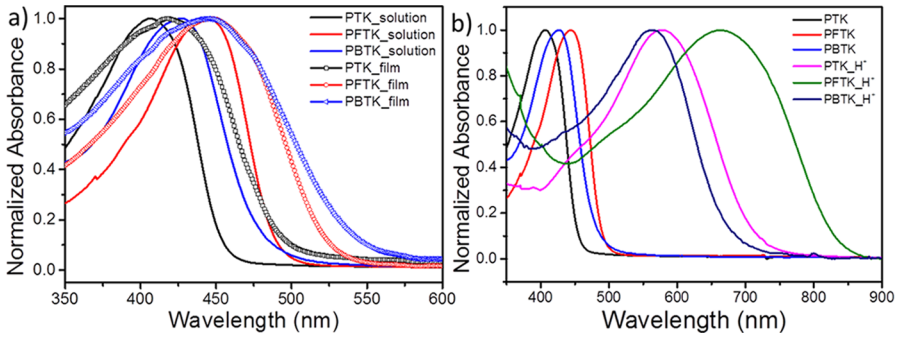

Figure 4. (a) Normalized UV−Vis absorption spectra for PTK, PBTK, and PFTK in the $CHCl_3$ solution and thin films. (b) Normalized absorption of aromatic polyketones as synthesized and when protonated with H_2SO_4.

2.3. Photophysical Properties. Figure 4a shows the UV−vis absorption spectra for the aromatic polyketones in the $CHCl_3$ solution and thin films. Their photophysical properties and the estimated optical band-gap are summarized in Table 2.

Table 2. Photophysical Properties Data of PTK, PBTK, and PFTK

polymer	$\lambda_{max}^{sol.}$ (nm)	λ_{max}^{film} (nm)	λ_{onset}^{film} (nm)	$E_g^{opt.}$ (eV)	$\lambda_{max}^{ems.}$ (nm)	Stokes shift (nm)
PTK	408	420	494	2.51	490	82
PBTK	428	445	526	2.36	541	113
PFTK	445	450	539	2.30	520	75

The maximum absorption peak of PTK, PBTK, and PFTK is at 408, 428, and 445 nm in $CHCl_3$, respectively, which is attributable to the characteristic absorption of the $\pi \rightarrow \pi^*$ transition of the polymer backbone. The maximum thin film absorption peak of PTK, PBTK, and PFTK is at 420, 445, and 450 nm, respectively. Compared with solution absorption, all aromatic polyketone thin-film absorptions show a red shift, indicating an enhanced interchain $\pi-\pi$ stacking in the solid state. According to the thin film absorption onset, the estimated optical band gaps of PTK, PBTK, and PFTK is 2.51, 2.36, and 2.30 eV, respectively, which indicates that inserting an electron donor or acceptor group can effectively reduce the band gap in this cross-conjugated system. Thus, despite being cross-conjugated, the tunable optoelectronic properties of aromatic polyketones mirror those of conventional, linear conjugated polymers.

We also acquired the absorption spectrum of protonated aromatic polyketones by treating them with H_2SO_4, as shown in Figure 4b. This protonation process is shown in Figure 5; protonation of the carbonyl units breaks the cross-conjugation by generating closed-shell carbocations in the conjugated backbone, converting the cross-conjugation to linear conjugation.[5−7,23] The net effect is to increase the conjugation length dynamically, which is reflected in a decrease in the band gap from 2.51 to 1.76 eV for PTK, 2.36 to 1.85 eV for PBTK, and 2.30 to 1.41 eV for PFTK. The mild electron-donating nature of fluorene stabilizes the carbocations, leading to the largest shift. The smallest shift occurs with PBTK, likely a due to the electron-withdrawing nature of benzothiadiazole. The photophysical properties of the polyketones in their protonated form is predictive of the properties of CPIs derived from them because protonation of the carbonyl oxygens results in the formation of (transient) carbocations in the backbone, which function as acceptors. Thus, the UV−vis spectra of protonated polyketones give insight into the donor−acceptor copolymer nature of the corresponding CPI. In this case, the donor character of fluorene interacts with the acceptor character of the diaryl carbocation, which is invariant across the series, to give the largest red shift, indicating that fluorene has the most donor character.

The steady-state fluorescence spectra of PTK, PBTK, and PFTK in $CHCl_3$ are shown in Figure 6a with steady-state emission peaks at 490, 541, and 520 nm respectively. Time-resolved fluorescence intensities are shown in Figure 6b. PBTK and PFTK clearly show mono-exponential photoluminescence decay with PBTK exhibiting the longest fluorescence lifetime of 745 ps while PFTK had a shorter lifetime of 500 ps. The photoluminescence decay of PTK, however, is bi-exponential, with lifetimes of 35 and 267 ps (see Figure S25 for fits). Interestingly, PTK shows a Stokes shift of 82 nm, while the Stokes shift of PFTK is only 75 nm, and PBTK exhibits the largest shift of 113 nm. These shifts are not consistent with the changes in absorption spectra, which indicates that the different aryl groups introduce significant conformational

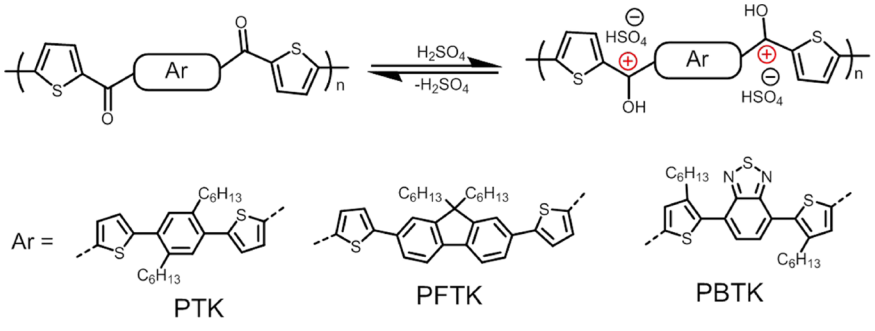

Figure 5. Protonation process in aromatic polyketones.

https://dx.doi.org/10.1021/acsomega.0c00223
ACS Omega 2020, 5, 4689−4696

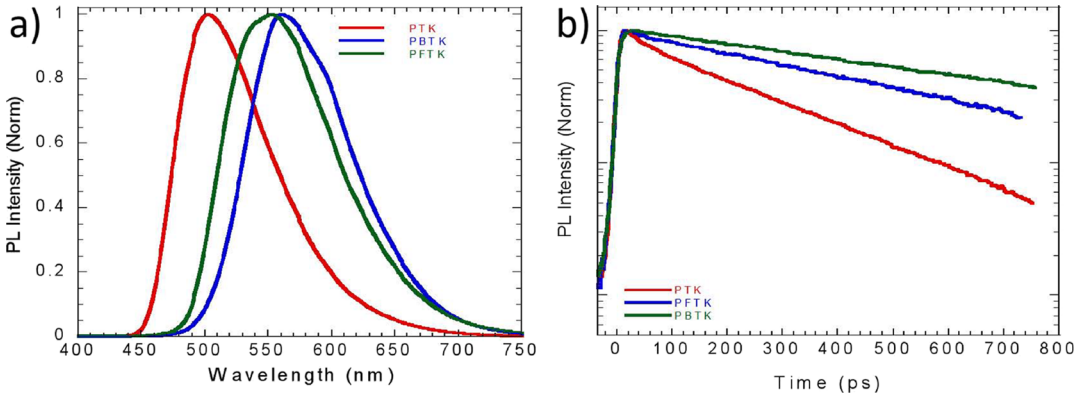

Figure 6. (a) Normalized steady-state fluorescence spectra for PTK, PBTK, and PFTK in the $CHCl_3$ solution. (b) Time-resolved fluorescence intensities of aromatic polyketone. PFTK and PBTK showed mono-exponential photoluminescence decay with PBTK exhibiting a lifetime of 745 ps and PFTK a lifetime of 500 ps. PTK showed bi-exponential photoluminescence decay with lifetimes of 35 ps and 267 ps.

flexibility, in agreement with the DSC measurements discussed above.

2.4. Electrochemical Properties. In order to gain an insightful understanding of the electrochemical properties of PTK, PBTK, and PFTK, the cyclic voltammetry (CV) characterization was carried out, and the results are shown in Figure 7. Half-wave reduction potentials and the estimated

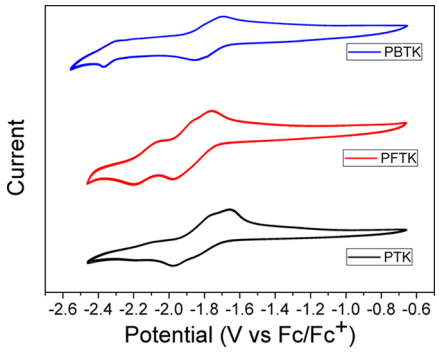

Figure 7. Cyclic voltammograms of aromatic polyketones (0.001 mol L^{-1}) in an ODCB−CH_3CN (9:1) solution containing a Bu_4NPF_6 (0.1 mol L^{-1}) electrolyte at a scanning rate of 100 mV s^{-1}.

Table 3. Electrochemical Properties Data and Molecular Energy Levels of PTK, PBTK, and PFTK

polymer	$E_{1/2}^{red}$ (V)	LUMO (eV)[a]	HOMO (eV)[b]	LUMO (eV)[c]	HOMO (eV)[c]
PTK	−1.81	−2.99	−5.50	−2.91	−6.30
PBTK	−1.76	−3.04	−5.34	−3.19	−6.26
PFTK	−1.86	−2.94	−5.30	−2.89	−5.91

[a]Calculated from CV: $E_{LUMO} = -(4.80 + E_{1/2}^{red})$ eV. [b]Calculated from E_{LUMO} and $E_g^{opt.}$: $E_{HOMO} = E_{LUMO} - E_g^{opt.}$. [c]The DFT calculation data.

LUMO levels of aromatic polyketones are listed in Table 3. Ferrocene/ferrocenium (Fc/Fc^+) was used as a standard reference, which was assigned an absolute energy of −4.8 eV versus vacuum. As expected,[4] all the aromatic polyketones exhibited two fully reversible reduction waves. The first half-wave reduction peak of PTK, PBTK, and PFTK are −1.81, −1.76, and − 1.86 V, respectively, relative to the redox potential of Fc/Fc^+. The LUMO energy levels of aromatic polyketones are calculated from the first half-wave reduction potentials using the equation $E_{LUMO} = -(4.80 + E_{1/2}^{red})$. The estimated LUMO energy levels of PTK, PBTK, and PFTK are −2.99, −3.04, and − 2.94 eV, respectively. The HOMO energy level was calculated based on the optical band gap and the LUMO energy level. The estimated HOMO energy levels of PTK, PBTK, and PFTK are −5.50, −5.34, and −5.30 eV, respectively. The LUMO energy level of PBTK is 0.1 eV lower than that of PTK, and the HOMO energy level is 0.16 eV higher than that of PTK. The LUMO energy level of PFTK is 0.05 eV higher than that of PTK, and the HOMO energy level is 0.2 eV higher than that of PTK. PBTK exhibited the lowest LUMO energy level, and PFTK showed the highest HOMO energy level, which indicates that the electron-deficient group (benzothiadiazole) can reduce the LUMO energy level and the electron-rich group (fluorene) can increase the HOMO energy level in these cross-conjugated polymers.

2.5. Density Functional Theory Calculation. To investigate the electronic structures, density functional theory (DFT) calculations were carried out at the B3LYP/6-311G(p) level using the Gaussian 16 program.[24] All polymers having two repeat units with the methyl substituent were used to reduce the calculation time. The optimized geometries for aromatic polyketones are shown in Figure S26. All polymers exhibit twisted gas-phase geometries, which might originate from the conformational flexibility link of the ketone unit. Compared to PTK, PFTK is more planar, and PBTK is more twisted. The calculated molecular frontier molecular orbitals are shown in Figure 8 and are summarized in Table 3. Twisted backbone geometries typically are unfavorable for charge delocalization and transfer; nonetheless, in PTK and PBTK, the HOMO is distributed across the entire backbone. While in PFTK, the HOMO is mainly localized on the fluorene moiety, only slightly extending to the thiophene unit. The LUMOs of PTK and PFTK are mainly distributed over the thiophene and ketone groups. The LUMO of PBTK is mainly localized on the benzothiadiazole unit, extending slightly to the thiophene and ketone units due to the electron-deficient nature of benzothiadiazole and ketones. Therefore, aromatic polyketones with the electron-deficient group (benzothiadiazole) show the lowest LUMO energy level, and electron-rich group (fluorene) show the highest HOMO energy level. These values are consistent with the electrochemical data, indicating that the calculations on short oligomers are a reasonable approximation for the polymers (in solution). Furthermore, the lower LUMO

https://dx.doi.org/10.1021/acsomega.0c00223
ACS Omega 2020, 5, 4689−4696

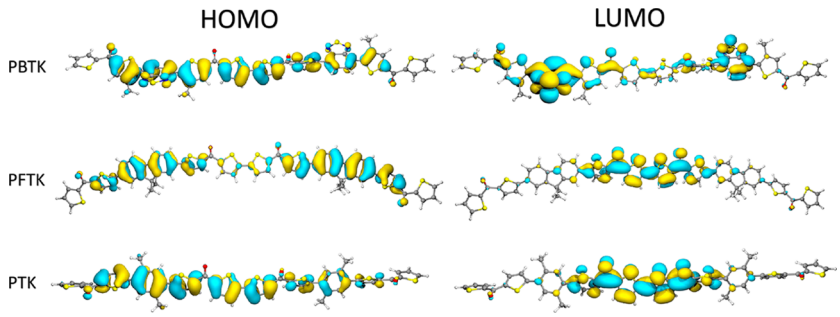

Figure 8. Calculated LUMO and HOMO for aromatic polyketones. The DFT calculations were performed at the B3LYP/6-311G(p) level using the program Gaussian 16.

of PBTK and higher HOMO of PFTK give rise to smaller band gaps compared with PTK, which accounts for the red shift observed in the absorption spectra.

3. CONCLUSIONS

In summary, we reported a new synthetic approach for the preparation of aromatic polyketones. This strategy shows a much larger substrate scope than the Friedel–Crafts polymerization methods previously employed. We were, therefore, able to prepare aromatic polyketones with electron-rich, neutral, and deficient units and to investigate their thermal, photophysical, and redox properties. In their neutral, cross-conjugated form, all polymers responded to the inclusion of electron-rich and electron-poor groups identically to linearly conjugated donor–acceptor polymers. Upon protonation, the carbonyl carbons become trivalent, extending the conjugation of the polymers dynamically. While the interest in aromatic polyketones is primarily as precursors to polymers with more interesting properties,[23] this work demonstrates that they posses useful properties on their own and sheds light on the role of cross-conjugation in band-gap engineering.

4. EXPERIMENTAL SECTION

4.1. Measurement and Characterization. ^{1}H and ^{13}C NMR spectra were measured using a Varian AMX400 (400 MHz) instrument at room temperature. NMR shifts are reported in ppm, relative to the residual protonated solvent signals of $CDCl_3$ (δ = 7.26 ppm) or at the carbon absorption in $CDCl_3$ (δ = 77.23 ppm). Multiplicities are denoted as: singlet (s), doublet (d), triplet (t) and multiplet (m). High-resolution mass spectroscopy (HRMS) was performed on a JEOL JMS 600 spectrometer. FT-IR spectra were recorded on a Nicolet Nexus FT-IR fitted with a Thermo Scientific Smart iTR sampler. GPC measurements were done on a Spectra Physics AS 1000 series machine equipped with a Viskotek H-502 viscometer and a Shodex RI-71 refractive index detector. The columns (PLGel 5 m mixed-C) (Polymer Laboratories) were calibrated using narrow disperse polystyrene standards (Polymer Laboratories). Samples were made in THF at a concentration of 1 mg mL^{-1} and filtered through a Gelman GHP Acrodisc 0.45μ membrane filter before injection. Thermal properties of the polymers were determined on TA Instruments DSC Q20, and TGA Q50 DSC measurements were executed with two heating–cooling cycles with a scan rate of 10 °C min^{-1}, and from each scan, the second heating cycle was selected. TGA measurements were done from 20 to 700 °C with a heating rate of 20 °C min^{-1}. UV–vis measurements were carried out on a Shimadzu UV 3600 spectrometer. Photoluminescence measurements were carried out on solutions contained in quartz cuvettes. The samples were excited by the second harmonic (approximately 400 nm) of a mode-locked Mira 900 Ti:Sapphire laser delivering 150 ps pulses at a repetition rate of 76 MHz. The laser power was adjusted using neutral density filters, and the excitation beam was spatially limited by an iris. The beam was focused with a 150 mm focal length in reflection geometry. Steady state spectra were collected by a spectrometer with a 50 lines/mm grating and recorded with a Hamamatsu em-CCD array. For time-resolved measurements, the same pulsed excitation source was used. Spectra were in this case collected on a Hamamatsu streak camera working in Synchroscan mode (time resolution 2 ps) with a cathode sensitive in the visible spectra. All plotted spectra were corrected for the spectral response of the setup using a calibrated lamp. Cyclic voltammetry (CV) was carried out with an Autolab PGSTAT100 potentiostat in a three-electrode configuration where the working electrode was platinum electrode, the counter electrode was a platinum wire, and the pseudo-reference was a Ag wire that was calibrated against ferrocene (Fc/Fc^{+}). Cyclic voltammograms of aromatic polyketones (0.001 mol L^{-1}) in an ODCB–$CHCN_3$ (9: 1) solution containing a Bu4NPF6 (0.1 mol L^{-1}) electrolyte at a scanning rate of 100 mV s^{-1}.

4.2. General Aromatic Polyketones Synthesis Procedures. All reactions were performed under anhydrous conditions under a nitrogen atmosphere. To a flame-dried flask containing a mixture of DMF:Toluene were added equal molar quantities of monomer and bis(pinacolato)diboron (**BiPi**). The solution was then purged with bubbling nitrogen for 10 min before the addition of 5 to 10 mol % 1,10-bis(diphenylphosphino)-ferrocenepalladium(II)dichloride dichloromethane complex $Pd(dppf)_2Cl_2$ and 5 equiv of crushed K_3PO_4, and the solution used a freeze-pump-thaw cycle technique to remove O_2, done three times. The reaction mixture was carried out to 110 °C and stirred overnight (about 15 h) and cooled to room temperature, and the solvent was removed by rotary evaporation. The remaining residue was dissolved in a minimal amount of $CHCl_3$ and precipitated by pouring slowly into a large excess of CH_3OH. The resulting slurry was stirred for an hour, and the precipitate was collected by filtration and then further purified by Soxhlet extraction with hexane, methanol, and chloroform, successively. The chloroform fraction polymer was collected. The purified polymer dissolved before being re-precipitated into cold CH_3OH and dried in vacuo.

4.3. Poly[(2,5-dihexyl-1,4-phenylene)bis(thiophene-5,2-diyl))bis(thiophen-2-ylmethanone)] PTK. K_3PO_4 (495 mg, 2.33 mmol), monomer **1** (367 mg, 0.467 mmol),

https://dx.doi.org/10.1021/acsomega.0c00223
ACS Omega 2020, 5, 4689–4696

BiPi (119 mg, 0.467 mmol), and $Pd(dppf)_2Cl_2$ (35 mg, 0.047 mmol) were reacted in 20 mL dry mixture solvents of DMF and toluene (1:1) according to the general aromatic polyketones polymerization procedure. Pure **PTK** (30 mg, 11%) was obtained as a yellow powder.

^{1}HNMR (400, $CDCl_3$) δ: 8.11−7.11 (m, 8H), 3.05−2.52 (m, 4H), 1.75−1.41 (m, 4H), 1.42−0.98 (m, 12H), 0.95−0.75 (m, 6H). **IR** (cm^{-1}): 22924, 2853, 1606, 1507, 1427, 1299, 1265, 1118, 1056, 892, 839, 811, 787, 722.

4.4. Poly[((9,9-dihexyl-9*H*-fluorene-2,7-diyl)bis-(thiophene-5,2-diyl))bis(thiophen-2-yl-methanone)] PFTK. K_3PO_4 (265 mg, 1.25 mmol), monomer **2** (219 mg, 0.25 mmol), BiPi (64 mg, 0.25 mmol), and $Pd(dppf)_2Cl_2$ (10 mg, 0.014 mmol) were reacted in 10 mL dry mixture solvents of DMF and toluene (1:1) according to the general aromatic polyketones polymerization procedure. Pure **PFTK** (40 mg, 23%) was obtained as a red powder.

^{1}HNMR (400, CDCl3) δ: 8.16−7.18 (m, 14H), 2.22−1.88 (m, 4H), 1.77−1.88 (m, 4H), 1.77−1.33 (m, 12H), 0.82−0.68 (m, 6H). **IR** (cm^{-1}): 2924, 2852, 1601, 1506, 1413, 1337, 1274, 1118, 1054, 889, 840, 803, 786, 721.

4.5. Poly[(benzo[*c*][1,2,5]thiadiazole-4,7-diylbis(4-hexylthiophene-5,2-diyl))bis(thioph-en-2-ylmethanone)] PBTK. K_3PO_4 (156 mg, 0.74 mmol), monomer **3** (125 mg, 0.15 mmol), BiPi (38 mg, 0.15 mmol), and $Pd(dppf)_2Cl_2$ (5 mg, 0.007 mmol) were reacted in 10 mL of dry mixture solvents of DMF and toluene (1:1) according to the general aromatic polyketones polymerization procedure. Pure **PBTK** (24 mg, 24%) was obtained as a red powder.

^{1}HNMR (400,CDCl3) δ: 8.14−7.13 (m, 8H), 2.98−2.49 (m, 4H), 1.85−1.51 (m, 4H), 1.42−0.98 (m, 12H), 0.93−0.68 (m, 6H). **IR** (cm^{-1}): 2922, 2853, 1600, 1529, 1507, 1424, 1298, 1270, 1194, 1090, 1049, 875, 836, 777, 722.

■ ASSOCIATED CONTENT

Supporting Information

The Supporting Information is available free of charge at https://pubs.acs.org/doi/10.1021/acsomega.0c00223.

Experimental details including synthesis procedures for monomers, the HNMR spectra, FT-IR spectra, GPC profile, full DSC curves, and partly UV−vis spectra of cross-conjugated polymers (PDF)

■ AUTHOR INFORMATION

Corresponding Author

Ryan C. Chiechi − *Stratingh Institute for Chemistry, University of Groningen, Groningen, AG 9747, The Netherlands; Zernike Institute for Advanced Materials, Groningen, AG 9747, The Netherlands;* orcid.org/0000-0002-0895-2095; Email: r.c.chiechi@rug.nl

Authors

Gang Ye − *Stratingh Institute for Chemistry, University of Groningen, Groningen, AG 9747, The Netherlands; Zernike Institute for Advanced Materials, Groningen, AG 9747, The Netherlands*

Yuru Liu − *Stratingh Institute for Chemistry, University of Groningen, Groningen, AG 9747, The Netherlands; Zernike Institute for Advanced Materials, Groningen, AG 9747, The Netherlands*

Mustapha Abdu-Aguye − *Zernike Institute for Advanced Materials, Groningen, AG 9747, The Netherlands*

Maria A. Loi − *Zernike Institute for Advanced Materials, Groningen, AG 9747, The Netherlands;* orcid.org/0000-0002-7985-7431

Complete contact information is available at: https://pubs.acs.org/10.1021/acsomega.0c00223

Notes

The authors declare no competing financial interest.

■ ACKNOWLEDGMENTS

This work is part of the research program of the Foundation for Fundamental Research on Matter (FOM), which is part of The Netherlands Organization for Scientific Research (NWO). This is a publication by the FOM Focus Group "Next Generation Organic Photovoltaics", participating in the Dutch Institute for Fundamental Energy. G.Y. and Y.L. acknowledge financial support from the China Scholarship Council (CSC). We would like to thank the Center for Information Technology of the University of Groningen for their support and for providing access to the Peregrine high-performance computing cluster.

■ REFERENCES

(1) Yonezawa, N.; Okamoto, A. Synthesis of Wholly Aromatic Polyketones. *Polym. J.* **2009**, *41*, 899−928.

(2) Yang, J.; Gibson, H. W. Polyketone Synthesis Involving Nucleophilic Substitution via Carbanions Derived From Bis(α-Amino Nitrile)s. 2. 1 Wholly Aromatic Polyketones Without Ether Linkages. *Macromolecules* **1997**, *30*, 5629−5633.

(3) Yang, J.; Gibson, H. W. A Polyketone Synthesis Involving Nucleophilic Substitution via Carbanions Derived from Bis (α-aminonitrile) s . 5 . 1-4 A New , Well-Controlled Route to " Long " Bisphenol and Activated Aromatic Dihalide Monomers. *Macromolecules* **1999**, 8740−8746.

(4) Chiechi, R. C.; Sonmez, G.; Wudl, F. A Robust Electroactive N-Dopable Aromatic Polyketone. *Adv. Funct. Mater.* **2005**, *15*, 427−432.

(5) Voortman, T. P.; Bartesaghi, D.; Koster, L. J. A.; Chiechi, R. C. Cross-Conjugated N-Dopable Aromatic Polyketone. *Macromolecules* **2015**, *48*, 7007−7014.

(6) Voortman, T. P.; de Gier, H. D.; Havenith, R. W. A.; Chiechi, R. C. Stabilizing Cations in the Backbones of Conjugated Polymers. *J. Mater. Chem.* **2014**, *2*, 3407−3415.

(7) Voortman, T. P.; Chiechi, R. C. Thin Films Formed From Conjugated Polymers With Ionic, Water-Soluble Backbones. *ACS Appl. Mater. Interfaces* **2015**, *7*, 28006−28012.

(8) McClain, M. D.; Whittington, D. A.; Mitchell, D. J.; Curtis, M. D. Novel Poly(3-alkylthiophene) and Poly(3- alkylthienyl ketone) Syntheses via Organomercurials. *J. Am. Chem. Soc.* **1995**, 3887−3888.

(9) Curtis, M. D.; McClain, M. D. Synthesis of Poly(3-Alkylthienylene Ketone)s by the PdCatalyzed Copolymerization of Carbon Monoxide With Thienyl Mercuric Chlorides. *Chem. Mater.* **1996**, *8*, 945−951.

(10) Curtis, M. D.; McClain, M. D. A New Poly(3-Alkylthiophene) Synthesis via Pd-Catalyzed Coupling of Thienyl Mercuric Chlorides. *Chem. Mater.* **1996**, *8*, 936−944.

(11) Hudson, L. G.; Stevens, M. P. Synthesis of Cross-Conjugated Polyketones by the Crossed-Aldol Condensation of Cyclic Ketones With Aromatic dialdehydes. *J. Polym. Sci., Part A: Polym. Chem.* **1995**, *33*, 71−78.

(12) Ito, S.; Wang, W.; Nishimura, K.; Nozaki, K. Formal Aryne/Carbon Monoxide Copolymerization to Form Aromatic Polyketones/Polyketals. *Macromolecules* **2015**, *48*, 1959−1962.

(13) Heeger, A. J. Semiconducting Polymers: The Third Generation. *Chem. Soc. Rev.* **2010**, *39*, 2354−2371.

(14) Yonezawa, N.; Miyata, S.; Nakamura, T.; Mori, S.; Ueha, Y.; Katakai, R. Synthesis of Wholly Aromatic Polyketones Using 2,2′-

Dimethoxybiphenyl as the Acyl-Acceptant Monomer. *Macromolecules* **1993**, *26*, 5262−5263.
(15) Yonezawa, N.; Ikezaki, T.; Nakamura, H.; Maeyama, K. Successful Synthesis of Wholly Aromatic Polyketones via Nickel-Mediated Aromatic Coupling Polymerization. *Macromolecules* **2000**, *33*, 8125−8129.
(16) Kanetaka, Y.; Yamazaki, S.; Kimura, K. Preparation of Poly(ether Ketone)s Derived From 2,5-Furandicarboxylic Acid via Nucleophilic Aromatic Substitution Polymerization. *J. Polym. Sci., Part A: Polym. Chem.* **2016**, *54*, 3094−3101.
(17) Kanetaka, Y.; Yamazaki, S.; Kimura, K. Preparation of Poly(ether Ketone)s Derived From 2,5-Furandicarboxylic Acid by Polymerization in Ionic Liquid. *Macromolecules* **2016**, *49*, 1252−1258.
(18) Rehahn, M.; Schlüter, A.-D.; Wegner, G. Pd-Catalyzed Polycondensation of Aromatic Monomers With Functional Groups. *Makromol. Chem., Rapid Commun.* **1990**, *11*, 535−539.
(19) Moore, J. S. Pd-Catalyzed Polycondensation of Aromatic Monomers With Functional Groups. *Makromol. Chem., Rapid Commun* **1992**, *13*, 91−96.
(20) Bochmann, M.; Lu, J. Synthesis of Poly(biphenylene Ketone)s via Palladium Catalyzed Crosscoupling Reactions With Ketone Diacetals. *J. Polym. Sci., Part A: Polym. Chem.* **1994**, *32*, 2493−2500.
(21) Brouwer, F.; Alma, J.; Valkenier, H.; Voortman, T. P.; Hillebrand, J.; Chiechi, R. C.; Hummelen, J. C. Using Bis(pinacolato)-diboron to Improve the Quality of Regioregular Conjugated Co-Polymers. *J. Mater. Chem.* **2011**, *21*, 1582−1592.
(22) Zhou, D.; Doumon, N. Y.; Abdu-Aguye, M.; Bartesaghi, D.; Loi, M. A.; Anton Koster, L. J.; Chiechi, R. C.; Hummelen, J. C. High-Quality Conjugated Polymers via One-Pot Suzuki-Miyaura Homo-polymerization. *RSC Adv.* **2017**, *7*, 27762−27769.
(23) Ye, G.; Doumon, N. Y.; Rousseva, S.; Liu, Y.; Abdu-Aguye, M.; Loi, M. A.; Hummelen, J. C.; Koster, L. J. A.; Chiechi, R. C. Conjugated Polyions Enable Organic Photovoltaics Processed From Green Solvents. *ACS Appl. Energy Mater.* **2019**, *2*, 2197−2204.
(24) Frisch, M. J.; Trucks, G. W.; Schlegel, H. B.; Scuseria, G. E.; Robb, M. A.; Cheeseman, J. R.; Scalmani, G.; Barone, V.; Petersson, G. A.; Nakatsuji, H.; Li, X.; Caricato, M.; Marenich, A. V.; Bloino, J.; Janesko, B. G.; Gomperts, R.; Mennucci, B.; Hratchian, H. P.; Ortiz, J. V.; Izmaylov, A. F.; Sonnenberg, J. L.; Williams-Young, D.; Ding, F.; Lipparini, F.; Egidi, F.; Goings, J.; Peng, B.; Petrone, A.; Henderson, T.; Ranasinghe, D.; Zakrzewski, V. G.; Gao, J.; Rega, N.; Zheng, G.; Liang, W.; Hada, M.; Ehara, M.; Toyota, K.; Fukuda, R.; Hasegawa, J.; Ishida, M.; Nakajima, T.; Honda, Y.; Kitao, O.; Nakai, H.; Vreven, T.; Throssell, K.; Montgomery, J. A., Jr.; Peralta, J. E.; Ogliaro, F.; Bearpark, M. J.; Heyd, J. J.; Brothers, E. N.; Kudin, K. N.; Staroverov, V. N.; Keith, T. A.; Kobayashi, R.; Normand, J.; Raghavachari, K.; Rendell, A. P.; Burant, J. C.; Iyengar, S. S.; Tomasi, J.; Cossi, M.; Millam, J. M.; Klene, M.; Adamo, C.; Cammi, R.; Ochterski, J. W.; Martin, R. L.; Morokuma, K.; Farkas, O.; Foresman, J. B.; Fox, D. J. *Gaussian~16*, Revision C.01; Gaussian Inc.: Wallingford CT, 2016.

https://dx.doi.org/10.1021/acsomega.0c00223
ACS Omega 2020, 5, 4689−4696